22/8/2016

Internship Report

Condition monitoring and testing of piezo elements for the activation of guided Lamb waves & damage identification using ultrasound scanning

Student: Daan te Molder (s1226029)

Location: Centre for Advanced Composite Materials (CACM), University of Auckland

Time: February – April 2016

Supervisors: Dr. Ir. R. Loendersloot,
Dr. Ir. M. Battley,
Dr. Ir. P. Kelly

Centre for Advanced Composite Materials

Student: Daan te Molder (s1226029)
Department: Centre for Advanced Composite Materials, University of Auckland
Mentors: Richard Loendersloot, Mark Battley & Piaras Kelly
Location: Auckland, New Zealand
Period: 6th February – 6th May
University of Twente, CTW, MS3, Richard Loendersloot

Preface

This report is written as part of my internship performed at the department of Centre for Advanced Composite Materials (CACM) at the University of Auckland during the months February – May. The internship is part of my master program, MS3, at the University of Twente. The internship was focussed on aspects related to the development of a structural health monitoring (SHM) technique utilizing guided Lamb waves for composite structures. I would like to thank my supervisors Richard Loendersloot (UT), Mark Battley (CACM, UoA), Piaras Kelly (CACM, UvA) for the organizational matters and practical, theoretical support at CACM during my internship. Also I want to thank the technician in the lab for helping with the experimental setup and providing all the tools.

Contents

1. Introduction

Structural components made out of carbon fibre reinforced plastic (CFRP) can be exposed to certain loading conditions which decrease the structural integrity without any visible damage on the outer shell. It is necessary to indicate these damages in order to guarantee the structure strength and performance during its lifetime. To locate small and invisible damages structural health monitoring (SHM) is from particular interest. With SHM the structural integrity is observed during its lifetime, without the need for destruction or taking parts out of operation. Ideally, parts are monitored continuously during full operation. This approach has the advantage that maintenance is only required if parts are significantly damaged and cause potential failure.

Industry has a growing interest in research dedicated to SHM, due to the increased demand for carbon fibre structures. Nowadays, inspection of carbon fibre parts is generally done using non-destructive testing (NDT) methods. A standard and accurate NDT method is ultrasonic scanning. Scanning the specimen visualises hidden delamination, voids or other defects inside composite structures utilizing an ultrasonic probe. However, these maintenance duties are time consuming and require parts to be out of operation.

Over the last decade, developments in the production techniques of carbon fibre parts resulted in bigger and more complex composite structures. These developments are beneficial for the overall structure integrity, although extra difficulties arise in condition monitoring. A promising new SHM approaches is developed for damage detection and localization, while the accuracy and identification can still be maintained by local ultrasound scanning. A comprehensive method description on the research dedicated to this method is written by Zhongqing Su & Lin Ye [1]. The so called acousto-ultrasonic method is based on the interference of propagating guided Lamb waves with defects or local changing material properties. Lamb waves [2] can cover long distances along a solid plate without much loss of signal strength, this unique capability is valuable for examining large areas and is applicable to a wide range of materials.

The Lamb wave method requires a broad network of actuators and sensors for the excitation and tracking of Lamb waves. A sophisticated way of lamb wave actuation is done utilizing piezo active wafer sensors (PWAS), these elements are relatively small and robust, they can actuate in the required frequency range and they can be integrated in the structure. Lastly, these elements can operate as actuator and sensor, due to this unique capability they have a strong preference above laser vibrometers, ultrasonic probes or other sensing methods. The PWAS elements are initiated by an alternating current, resulting in a vibration of the piezo patch at a certain frequency, which activates the Lamb wave to propagate through the specimen. The Lamb waves then travel through the panel and arrive at other PWAS elements, these elements output an electrical signal representing the lamb wave.

A network of sensors over the entire surface forms the base for the detection and localization of small defects, correlation analyses between baseline signals and signals gathered after several load cycles show defects. In figure 1 a simple set up is shown to clarify the method description. Damages as indicated in red can be localized by looking at all different trajectories individually. For example, the trajectory between piezo 1 and 5 will be affected by the presence of the defect. This method is a promising and efficient tool for damage detection [3] without the need of complicated or expensive equipment.

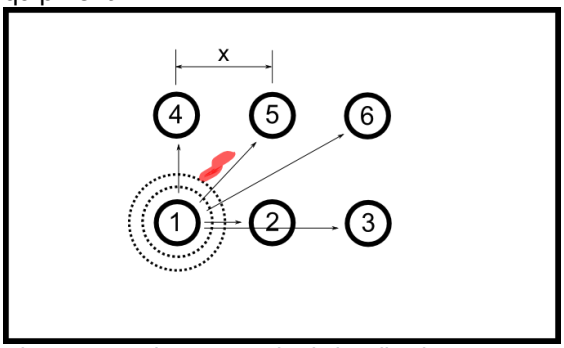

Figure 1: Lamb wave method visualisation

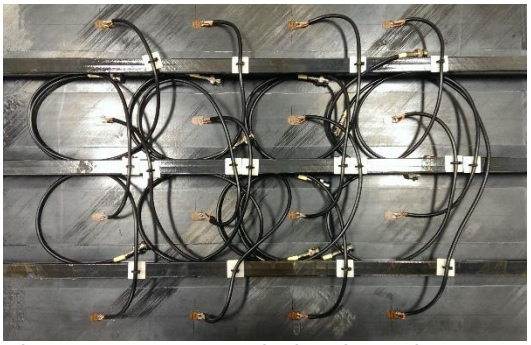
Figure 2: Sensor network aircraft panel

2. Motivation & Objectives

In literature the principle of this SHM approach is already proven, however a deeper understanding of all parameters is needed for the implementation in industry purposes. This report focusses on getting a deeper understanding of several aspects related to this SHM approach and is a extension to the research conducted by Loendersloot. In that particular research an aircraft panel (figure 2) is used to test the functionality of this approach. The aircraft panel is made out of a CFRP panel, with 3 stringers attached to the bottom side in the length direction. This aircraft panel is also referred to later in this report. In order to test this SHM approach on the aircraft panel, a defect is created by a controlled impact load. In this report the defect is investigated and characterised by making use of standard ultrasound technology. Besides the ultrasound scanning also other aspects have been treated. All aspects addressed in this report are briefly discussed next.

PWAS size

A wide variety of PWAS sensors is available on the market, the sensitivity is an important parameter and is related to the electro mechanical coupling factor of the piezo material. Low priced elements made of low priced materials are outperformed by the high priced elements. Although, no specific minimum requirements for the activation of lamb waves are stated in literature. Research dedicated to the performance of low priced PWAS elements is needed to form a basis for further research involving experimental set ups. Experiments are conducted to investigate the influence of size by the activation and sensing of guided lamb waves utilizing low-priced PWAS elements.

Non-linear structures & Sandwich material structures

The design freedom is also one of the main reason for the increased usage of CFRP materials. As result, a lot of CFRP material parts are curved or contain non-linear features. An important aspect in the development of this SHM method is the applicability onto non-linear geometries. Curvature or corners may contain high stress concentration and therefor it is important to ensure the integrity of this method for these designs. In this report, a curved specimen is tested for the propagation of Lamb waves. Besides curvature, the effectiveness of this method can also be limited by the material structure. For example, sandwich materials structures with a high acoustic impedance core will damp the propagation of the wave. Experiments have been conducted to point out the effect of non-linear geometries and different materials structures on the guided Lamb wave propagation.

Self-diagnostic PWAS element method

The integrity of this SHM method depends on the controllability of all conditions during the measurements in order to guarantee the reliability of the outcome. False damage detection can be the result of changing boundary conditions. Important issues are the bonding of the PWAS elements to the panel surface and the element condition itself. Debonding of a PWAS element for example can result in different wave activation. A self-diagnostic method, based on the susceptance, is tested by experiment to identify changing conditions. This self-diagnostic method is used to determine the condition of the PWAS elements on the aircraft panel.

Ultrasound scanning

The SHM method is valuable for damage detection and localization, the next step is the identification of the damage. Identification by ultrasound scanning is an important step, this characterizes the size of the defect and indicates if there is an emerging structure failure. Based on the defect size and characteristics, operators can decide whether it is necessary to repair, replace or leave it. To prove the validity and reliability of the experiments conducted with the aircraft panel, it is of importance to clearly identify the damage. An impact load is applied to the aircraft panel to create a defect in the structure. Ultrasound scanning is used to identify the impact load damage on the aircraft panel.

3. PWAS element size performance

Technical introduction and approach

There is an infinitely set of Lamb wave modes. The two wave modes to distinguish are the symmetric (S_i) and the anti-symmetric (A_i) wave mode (figure 3). The S_0 mode is known for its higher propagation speed compared to the A_0 wave mode[4]. A graph presented by Lowe [5], describes which modes become active at a certain frequencies. In other words, the graph (figure 4) shows which wave modes are generated and their wave velocity for different excitation frequencies. For the activation of lamb waves in composite structures, typical excitation frequencies of 20 – 500 kHz are used. The graph is useful to acquire proper wave activation in an experimental setup.

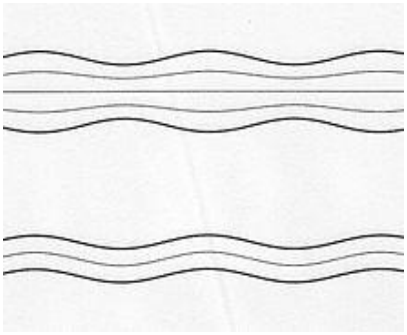

Figure 3: Symmetric (S) and anti-symmetric (A) Lamb wave modes

Theoretically, if the material is continuous infinite homogenous the wave slowly attenuates in magnitude while it propagates at a certain velocity [1]. However, in practise this is never the case. Free boundaries, damages or geometrical non-linearity's influence the wave propagation. The influence of a defect on the wave propagation is unique and hard to predict. Research on guided lamb waves crossing a delamination in a composite structure is described in a paper by Kim [6]. In this paper, delamination's of different layup settings and thicknesses are analysed. It shows that defects can be recognised by extra reflections returning to the sensors. Changing layup orientations results in different reflections.

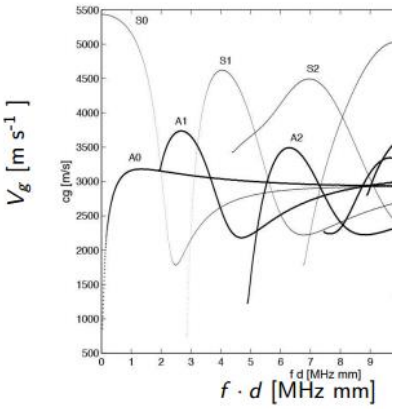

Figure 4: Wave mode velocity

Accordingly, defects are detected based on the presence of additional reflection or by changing wave forms. Therefor it is important that the Lamb waves have a considerable amplitude to acquire a high signal to noise sensor output. Preferably, the A and S wave mode arrive separately with a small time interval. Essentially, this all comes down to balancing between mutual distance, actuation frequency and voltage output. This is an important aspect for the application in industry. Therefor different material specimen are tested to get an indication of the wave propagation, with the goal to predict lamb wave behaviour in future research utilizing similar materials.

PWAS elements come in a wide variety, size, shape, frequency range, material etc. all affect the performance of these elements in the SHM experiments. In this report different sizes of low-priced piezo elements are tested. The applicability and sensitivity are evaluated for different sizes. Based on these results the PWAS elements are ordered for further experiments.

The experiment discussed in the next paragraph is conducted to determine what size of piezo element is best for lamb wave activation. Based on these results extra PWAS elements were ordered, to test for different material structures and geometries. Note that for both systems the same experimental setup is used, only the specimen is changed.

Methodology

The test strip contains 4 PWAS elements, 2 small (14.22mm) and 2 big sized (25.36) PWAS elements settled either at one side of the strip. The boundaries of the surface are covered by tacky tape to supress reflections of the boundary. The setup is shown in figure 5. The distance between the elements is 20 cm.

Each of the piezo elements is activated in sequence, while the others are used as sensors. For example, when PWAS 1 is used as actuator, the other 3 elements (nr, 2, 3, 4) serve as sensors and so on. In this particular case, the initiated Lamb wave travels from the actuator (PWAS 1) through the strip to PWAS 2 and 3.

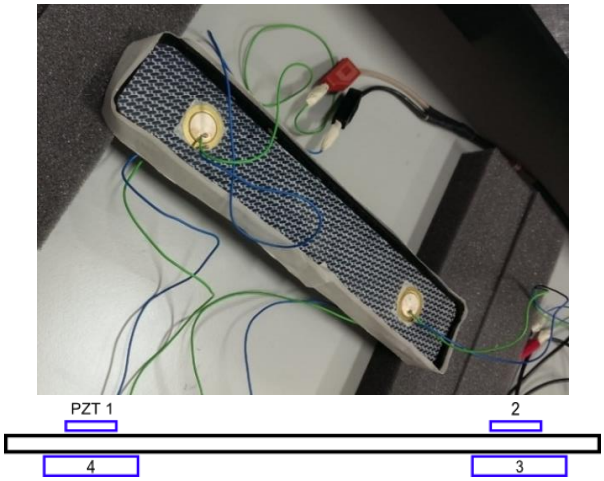

Figure 5: Test strip

All piezo elements are connected to a Handyscope system (Figure 6) [7], which produces the signal output for the activation of the piezo and collects the measured data. The handyscopes are controlled by a matlab program run from an external PC.

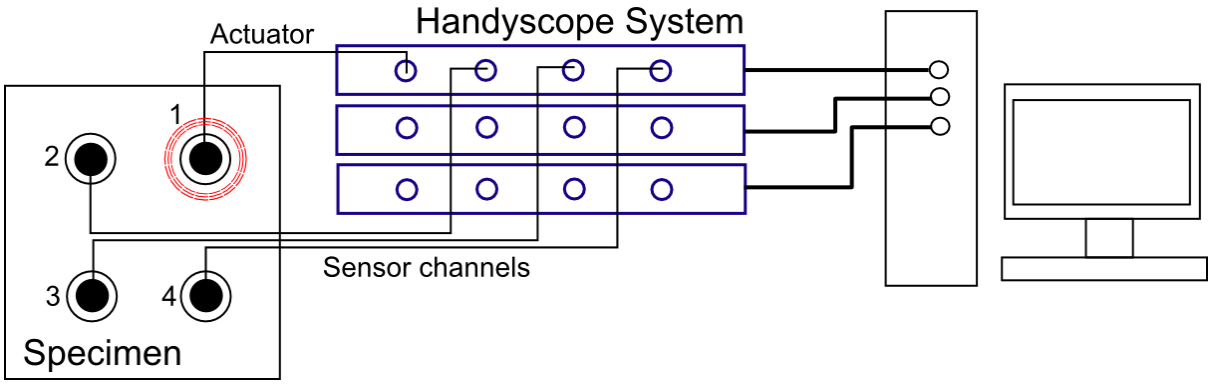

Figure 6: Handyscope system

The signal sent to the PWAS element is an electrical burst shaped signal (Figure 7) of a single frequency and maximum voltage output of 10V. This electrical signal is converted into a vibration by the PWAS element which triggers the guided Lamb wave. The Lamb waves arriving at the PWAS elements at the other end, cause an electric output. The electric output is recorded by the handyscope and sent the external PC for further analyses. To reduce the influence of external vibrations, the sensor data is averaged over 10 experiments.

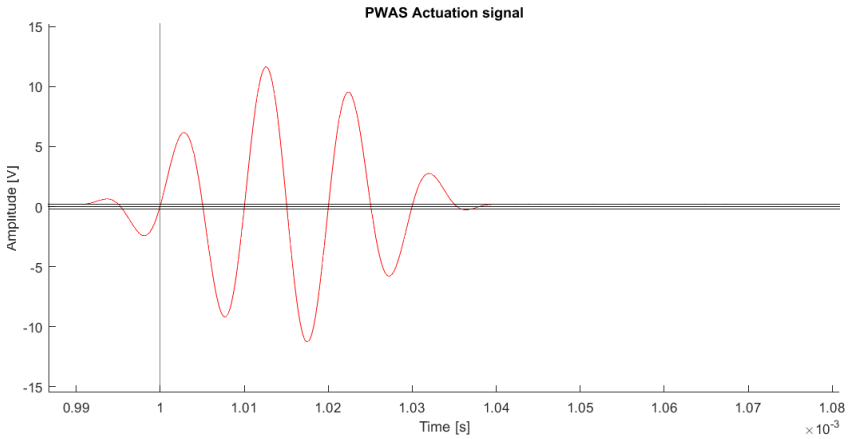

Figure 7: Acutuation signal (burst)

Test & performance parameter

After the test, all the sensor data of all frequencies is processed. The time domain data shows the electrical output of the PWAS element of each experiment. First the envelope plot over the time domain data is made. Then the maximum amplitude of the envelope at each frequency is collected and presented in one graph. This graphs shows at which frequencies the Lamb waves have the highest amplitude. A high amplitude indicates a strong Lamb wave, this is ideal for damage detection. The PWAS element is activated in the frequency range of 20 kHz till 100 kHz, with a 5 kHz stepsize. The frequency is taken as the variable and the maximum sensor amplitude is used for analysing the performance.

Results

The measured sensor data, is the time domain data as shown in figure 8, in this case the two receiving elements are number 1, 4. Figure 8 shows both the envelope plots, for the particular case of 100 kHz and actuator element 2. In the figure the light blue line indicates the sensor signal from big piezo, the darker line is the sensor signal corresponding to the smaller piezo. Although the boundaries taped, there is still a small reflection from the free boundary visible. At lower frequencies (70 kHz), the A_0 mode is significantly higher. At higher frequencies the S mode is dominant. Also interesting is that for higher frequencies, about 100 kHz, the S_0 and A_0 mode arrive at the same time. Increasing the mutual distance should lead to a clear separation of the wave modes, since the A mode is supposed to have a lower wave velocity. Only the strip is too short to test for increasing distance.

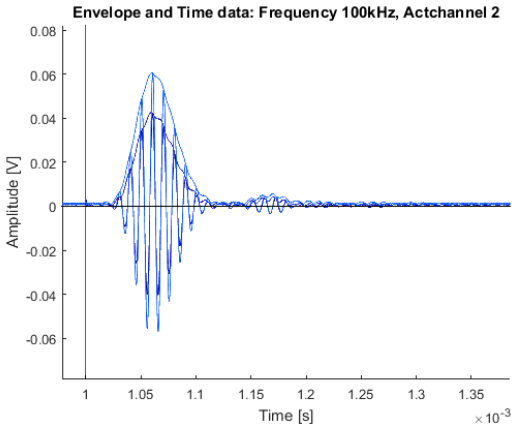

Figure 8: Envelope plot 100kHz

The maximum amplitude for each frequency is shown in figure 9 and 10. In the left figure, the lamb waves are activated by a small PWAS element (14mm). It shows that for higher frequencies, the lamb waves have a higher amplitude.

In the right figure, the lamb waves are activated by a big PWAS element (25mm). The graphs shows that only for frequencies below 35 kHz the Lamb waves are activated properly.

It can be concluded that smaller piezo elements perform better for the activation of Lamb waves on this CFRP strip, with a maximum voltage of 10V. An increase in PWAS element diameter deteriorates the sensibility of high frequency Lamb waves.

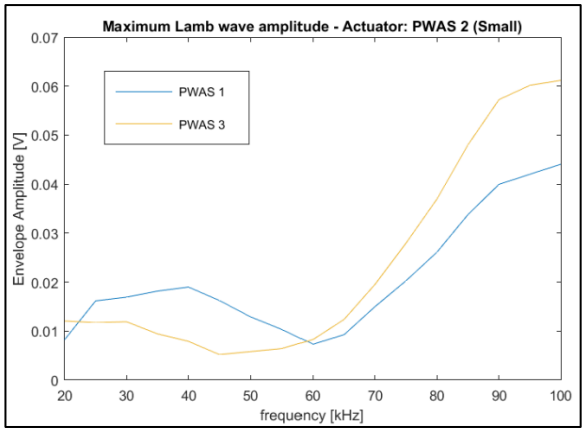

Figure 9: Envelope Amplitude, Actuator element 2 (small)

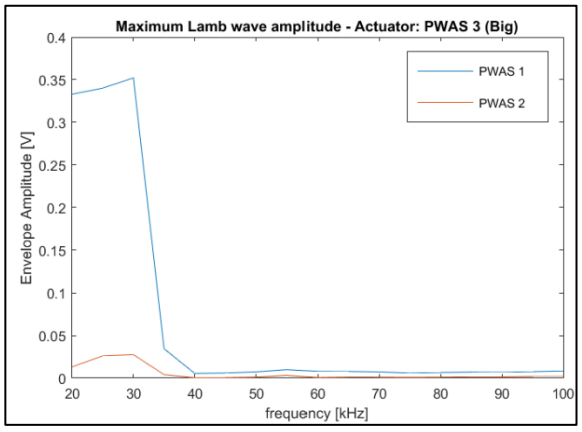

Figure 10: Envelope Amplitude, Actuator element 3 (big)

4. Guided Lamb waves propagation

Methodology

CFRP strip

Based on the results from previous experiments, extra 12mm Murata piezo electric elements are ordered for further research. The performance of these elements is tested by mounting them onto a CFRP strip. The strip, 6.2 mm thick and 465 mm in length is used. The relatively long length, make this strip suitable for analysing wave propagation. The PWAS elements are orientated as shown in figure 11. The mutual distances between PWAS elements ranges from 40 up to 370 mm to test for attenuation with different path lengths. The same handy scope system is used as presented in previous paragraph. The actuator signal frequency range is now 60 – 500 kHz with a 5 kHz stepsize.

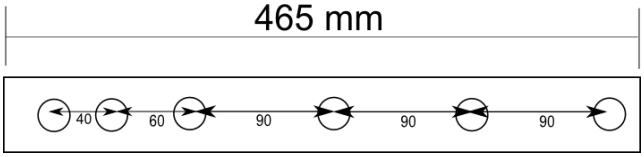

Figure 11: DLR strip test layout

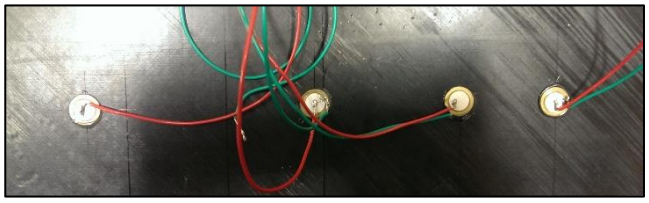

Curved CFRP specimen

The second specimen has a curvature, hence it is non-linear in geometry. The specimen is a small CFRP section out of a sailing boat mast, thus, this specimen could actually be a potential future application. The orientation of the PWAS elements on the structure is shown in the Figure 12. Only PWAS element 1 is used as actuator, elements 2, 3 and 4 are used as sensors. The mutual distance between the elements is 40mm.

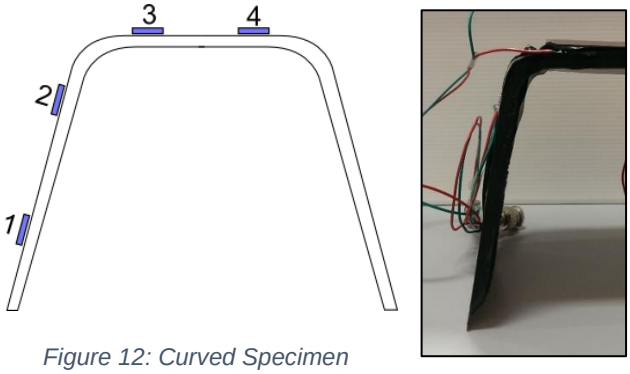

Figure 12: Curved Specimen

Sandwich material specimen

The third specimen is a sandwich material consisting of two glass fibre skin panels and a stiff foam structure core. 3 PWAS elements are placed on the top skin and 1 on the bottom skin to check if the Lamb wave is propagating through the material thickness. On the top skin the mutual distance varies between 30 to 50 mm.

Figure 13: Sandwich specimen: two glass fibre skin and foam core

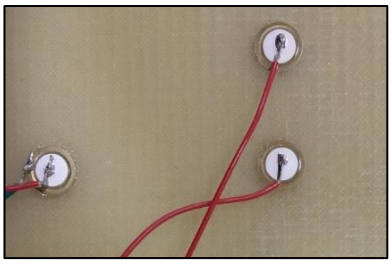

To test which actuation frequency is the best for activating lamb waves, the same analyses method is used as in the first experiment. This is done by taking the maximum measured electrical amplitude of the PWAS element (sensor) at each frequency. A high electrical output means a strong guided lamb wave. The maximum electrical amplitude of the PWAS element at each frequency is plotted in the graph. Again the average is taken over 10 experiments to exclude external influences.

Results: Signal attenuation analyses

CFRP strip

The 6.2 mm panel is tested for the frequencies 50 kHz up to 500 kHz, the graph (figure 14) shows two peaks, a small peak at 70 kHz and one around 300 kHz. Plotting the time domain showed that for low frequencies (50-100 kHz) the A-mode is most active. However, at high frequencies it is different. Especially around 300 kHz (figure 15) a strong S-mode is followed by a strong A-mode. Two strong modes have a great potential for damage detection.

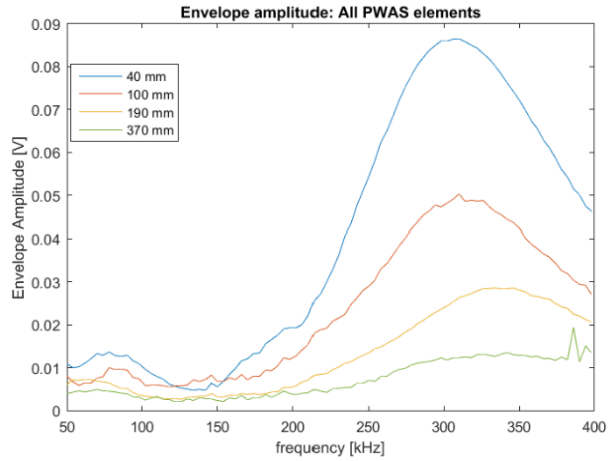

Figure 14: CFRP flat panel

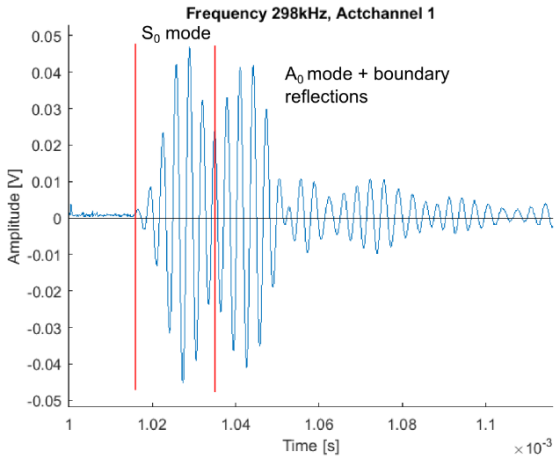

Figure 15: Time data CFRP flat panel

Curved CFRP specimen

Figure 16 shows that the wave propagation in the curved specimen is more attenuated. Sensor 2 at 40 mm, positioned before the curvature, shows a significantly stronger peak as sensor 3 at 80mm after the corner section (figure 12). Thus, the non-linear section has a high attenuation ratio. This is in contrast to the flat panel case where the attenuation is approximately linear over the distance. The time domain graphs made clear that the S-mode is mostly attenuated by passing the corner section, while the A-mode is less affected.

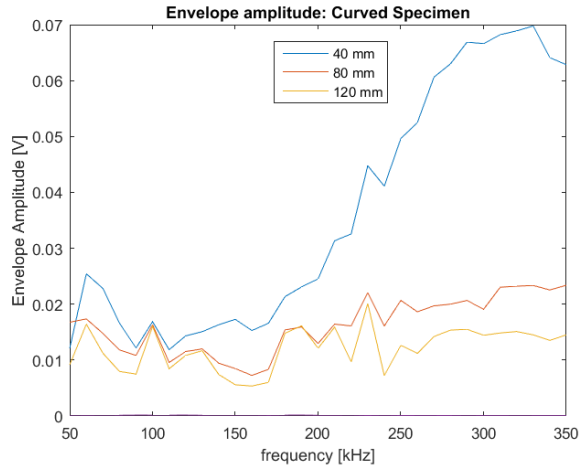

Figure 16: Curved specimen (mast section)

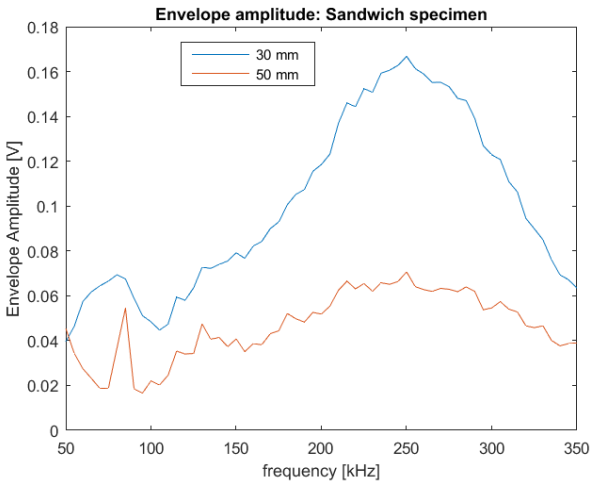

Figure 17: Sandwich panel

Sandwich material specimen

In the sandwich panel test the A-mode is almost completely disappeared. Although, the S mode appears to be less attenuated compared to the CFRP specimens. Figure 17 shows the envelope amplitude at different frequencies. Interesting is the maximum amplitude measured in the sandwich panel test, about 0.17 V at 250 kHz, is almost double the maximum amplitude measured in the CRFP specimen. According to the technical introduction, the A mode is an out of plane motion while S-modes move in plane. Out of plane motion is expected to be more damped by the core structure, this could declare the absence of the A-mode. The PWAS element placed on the bottom skin did not show any signal output, the wave is completely attenuated when crossing the foam layer.

5. PWAS self-diagnostics

Technical introduction

For structural health monitoring utilizing PWAS elements, it is necessary that the integrated sensors are under constant conditions during all measurements. Degradation, debonding or temperature of the elements can influence the sensor data, resulting in false damage identification. In literature, the electrical impedance of the piezo elements is proven to be a useful feature for testing the condition of a piezo and/or damage identification in the host structure [8]. This principle is based on the admittance/impedance, which consists of two characteristics, the mechanical impedance of the PWAS ($Z_a(\omega)$) and the host structure (panel) impedance ($Z(\omega)$). The total electrical admittance is described by the relation below. The admittance is the inverse of the impedance.

To show why the admittance is useful for the estimation of the condition, a short introduction is added about the modelling of an equivalent electrical circuit for PWAS elements. The Van Dyke Model (figure 18) is the most basic model approach [9], the capacitor describes the electro static capacitance of the piezo material and the RLC representing mechanical damping, mass and elastic compliance. The admittance is frequency dependent. Beyond the resonance frequencies, the piezo element is best approximated by just a single capacitor.

For unmounted piezo elements at resonance frequencies, the model is dependent on the capacitance and the piezo physical structure. Surface mounted PWAS involve a lot more parameters, since the host structure is now connected to the piezo structure. The resonance frequencies of the host structure are added to the model, this is achieved by adding extra RLC in parallel to the Van Dyke model. The model is proven to be a good approximation of the reality [9] and shows the usefulness of evaluating the admittance of the circuit to monitor the PWAS elements.

$$Y(\omega) = i\omega a\left(\epsilon_{33}^{T} - \frac{Z(\omega)}{Z(\omega) + Z_a(\omega)} d_{3x}^2 Y_{xx}^{E}\right)$$

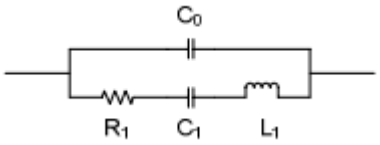

Figure 18: Van Dyke Model

The electrical admittance of the PWAS element is influenced by the combination of the host structure condition and the PWAS element condition itself [8], if one changes over the time the outcome will be affected. To monitor just the PWAS element condition and preclude the influence of the host structure, these measurements have to be distinguished. For the damage identification in the host structure, the impedance is more sensible, while the imaginary part of the admittance is more sensitive to PWAS element failure. Debonding, breakage and degradation of the sensors are the defects related to PWAS element failure. Breakage and degradation affect the capacitive value of the piezo material, therefor it is useful to only track the susceptance of circuit. The susceptance is the imaginary part of the admittance. It is proven that bonding layer changes are also easier to identify in the susceptance curve over the frequency [10]. The admittance is the inverse of the impedance. The impedance is defined as the voltage over the PWAS element, divided by the current over the PWAS element and results in a complex number.

Monitoring based on susceptance curves can be accomplished in several analysing methods according to literature [11]. It is found that correlation coefficient between the pristine (‘undamaged case’) and damaged case is a good condition indicator. However, the PWAS element condition is also influenced by temperature [11], therefor constant test condition have to be ensured at all times. A different method is analysing the correlation of a batch PWAS elements. This method is proven to be an efficient method for damage identification of the PWAS elements, since no baseline data, temperature or operation parameter control is required.

Methodology

The impedance measurement is obtained by applying a frequency sweep in the range of 0.1 - 1MHz with a maximum voltage amplitude of 10V. A small electrical circuit (figure 19) is used to determine the voltage and the current over the piezo element, these are needed to acquire the impedance value. The power source, the PWAS element and the resistor are in series, hence the voltage over the PWAS element is determined by subtracting the power source voltage by the resistor voltage. The current is acquired by measuring the voltage over a low ohm path, a composition resistor of 20 Ohm's is used in the experiment. The resistor has a low value such that the voltage drop at the resistor is minimal.

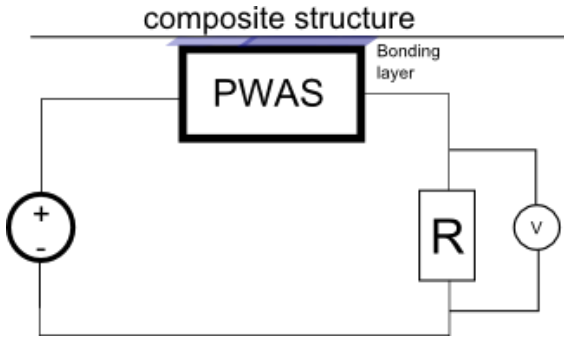

Figure 19: Electric circuit

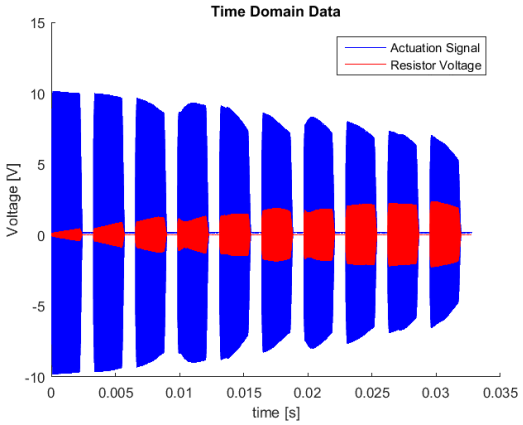

Figure 20: Time data frequency sweep

The time domain data is the direct result of the experiment (Figure 20). In the figure the actuation signal (blue) and the resistor voltage (red) is shown. Due to a small storage capacity in the Handyscope, 10 different sweeps are applied in sequence, each activating a different frequency range. When all the sweeps are conducted and the time domain is converted into the frequency domain by a fast Fourier transform, the data is merged together. Finally one data set is left containing all relevant data over the entire frequency range. The same handyscope system as in previous experiments is used, only is now connected to the electrical circuit to measure the resistor and power source voltage. The burst signal is replaced by the frequency sweep signal as shown in the figure.

Composition resistors normally decrease in resistance for higher frequencies, which is not the case. Possibly, the skin effect of the coax cables starts to interfere at higher frequencies. Also, the voltage drop in the actuation signal for higher frequencies is undeclared. When using unshielded wires, this effect became stronger. For the analyses this is not a problem, since all piezo elements are measured with the same circuit and are exposed to the same resistance, hence the error is consistent for all elements.

To minimize external influences on the signal, the average is taken over 10 experiments. The impedance (Z) is calculated by the formula given below, the inverse of the impedance is the admittance (Y) and the imaginary part of the admittance is the susceptance (B). All the results are as a function of the frequency.

$$Z(\omega) = \frac{U_{pwas}(\omega)}{I_{pwas}(\omega)}, \qquad Y = \frac{1}{Z}, \qquad B = imag(Y)$$

To identify different PWAS element failure mechanisms, several PWAS elements are tested by mounting them onto a 4.2 mm thick CFRP plate. The first damage scenario to analyse is the difference in bonding. The bonding layer between the PWAS and the composite structure is an epoxy glue. Gluing manually resulted in different layers of glue. Some elements covered in a thick layer of epoxy other elements are relatively loose. One sensor (PWAS 2) is covered in a thicker layer of glue to be completely integrated to the structure, called over bonding. Debonding is simulated by another sensor (PWAS 6), which has a smaller adhesive layer diameter than the average PWAS elements bonding layers. The case of breakage is simulated with two unsupported piezo elements, one pristine element and one broken element. After the identification of different sensor failure mechanisms, the characteristics are compared by the susceptance curves of the piezo elements mounted on the aircraft panel. The

characterization of each type of sensor failure is used to declare the results found by the susceptance measurements of the aircraft panel. The piezo elements in these test are different as the once integrated in the aircraft panel. Murata 12mm piezo electric elements are used for damage scenario analyses.

Results: Damage scenario Analyses

The breakage scenario is tested with two unsupported piezo elements, one pristine and one broken, resulting in a different gradient. In figure 22, the two cases are plotted. Note that the broken piezo has a lower gradient. This corresponds to the literature [11], a broken piezo has a lower capacitance and this leads to a decrease in slope.

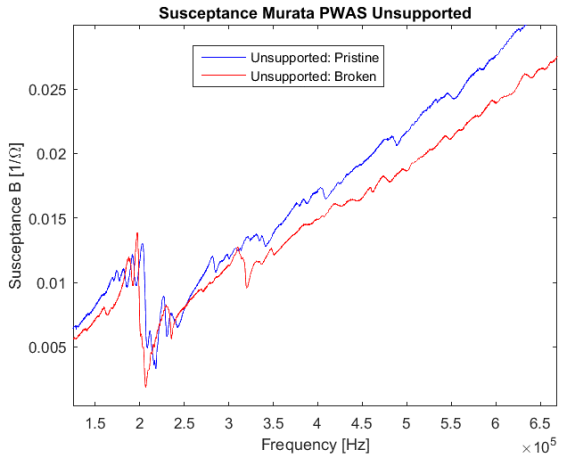

Figure 22: Pristine and broken PWAS element susceptance analyses

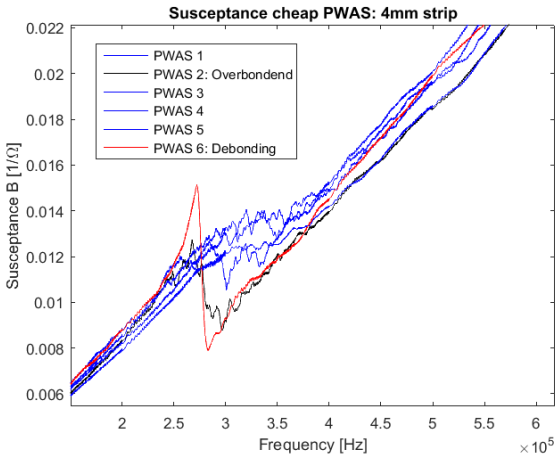

Figure 23: 4.2 mm strip susceptance analyses

For the sensor bonding failure two different scenarios are tested, the over bonding and lose bonding case. These scenarios are compared with 4 properly bonded piezo elements. The susceptance curves of all elements are plotted in figure 23. The effect of changing bonding layers, tends to show a change at the resonance frequency. In case of loose bonding (red line), there is strong anti-resonance peak to be recognized, as can be seen in the figure. The element covered in a thicker layer of glue (black line) did not change much, only a slightly stronger peak at the resonance frequency, but no anti resonance peak.

For comparison also the impedance, admittance and susceptance graphs in the frequency domain of a single PWAS is shown in figure 21. First thing to notice is that the impedance and admittance curve are similar, except for the resonance peak heights. At lower frequencies, the impedance is resonating

According to the technical introduction, the best feature for piezo monitoring is the susceptance, this theorem was reconfirmed by analysing the admittance curves of several elements. The real part of the admittance did not show any difference when suffering from element damage. Although, the imaginary part of the admittance did, which is known as the susceptance. Therefore, the susceptance is used for the PWAS condition determination on the aircraft panel.

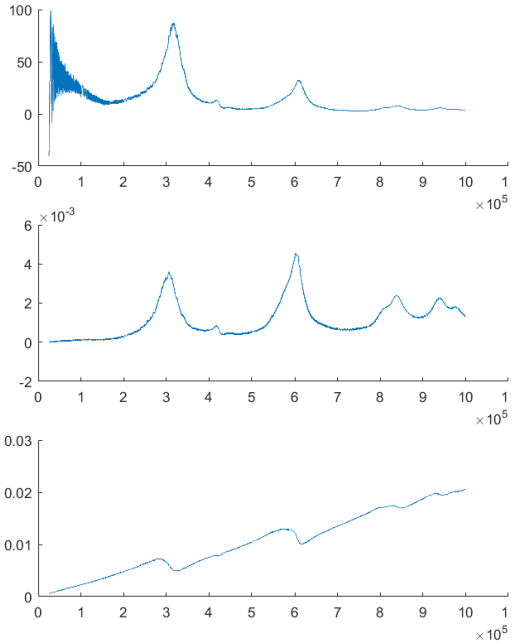

Figure 21: Impedance, Admittance, Susceptance

Results: Aircraft panel PWAS elements

The integrated sensors in the aircraft panel are tested after the impact damage application, no data was measured prior to the impact. The susceptance graphs are presented in figure 24. Apparently, most of the PWAS elements have a high correlation. Some PWAS elements on the aircraft panel show slightly different behaviour. Especially PWAS 5, 12 which are presented by green lines in the bottom of the figure. These PWAS are not properly connected and are excluded from further analyses. The peaks according to PWAS 2 (red) and 9 (black) are at different frequencies. These results correspond to the susceptance characteristics found in the damage scenario analyses. In figure 24, the encircled area shows the susceptance change most clearly. A small change in resonance frequency and the presence of a tiny resonance peak indicates that PWAS 2 and PWAS 9 are debonded/loose bonded from the panel surface.

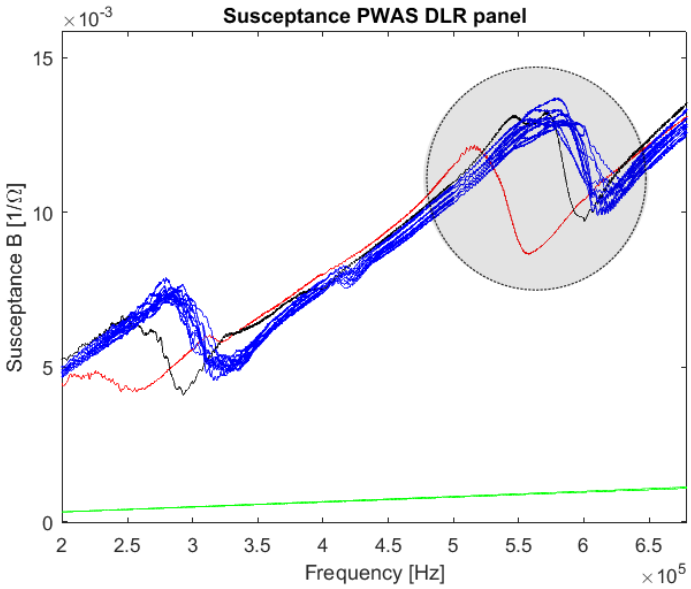

Figure 24: PWAS susceptance DLR panel

A closer look at the PWAS element bonding layer on the aircraft panel reveals the potential problem. Sensor 2, shown in the left image has a different orange tint along the edges as the healthy PWAS element shown in the right figure. This coulour change at the edges probably indicates less adhesive material (glue), resulting in debonding. PWAS 9 has similar appearances.

Figure 25: Aircraft panel PWAS 2 (left) & 9 (right)

6. Ultrasound scanning

Technical introduction

A standard way of non-destructive testing (NDT) of composite materials is ultrasound scanning technology. The purpose of ultrasound technology is basically to obtain information about the material composition based on the analyses of an ultrasonic sound wave travelling through solid material. The ultrasound wave is activated by a probe, it propagates through the material with a certain acoustic pressure and acoustic impedance. The wave energy is partially reflected, an “echo”, by the presence of a defect, causing an impedance mismatch. A high impedance mismatch, results in a strong reflection. The formulas below give a value for the acoustic impedance, ρ is the density of the specimen and C_l is wave velocity. The last formula gives an indication for the fraction of the energy that is reflected [12]. For example the reflection approaches 100%, if the transition is between steel and air. Typical frequencies for ultrasound scanning is in the range of 1 MHz up to 20 MHz

$$Z = \rho\, C_l\,, \qquad R = \frac{Z_2 - Z_1}{Z_2 + Z_1}$$

Ultrasound scanning is usually applied for the inspection of metal structures, to inspect welt quality or finding cracks. Non homogenous materials as composites are less ideal for ultrasound scanning, signals are more influenced by noise. However, research proved that imperfections can clearly be observed since the reflection energy is still significantly higher as the noise content.

Standard ultrasonic devices have one single probe, phased array probes consist of a series of probes integrated into one head. Multiple probes offer the possibility of beam angle steering and 2D imaging, resulting in better scanning quality and images. The beam can be focussed on specific depths or angles which gives a more clear characterization of the imperfection/defect. Beam steering is accomplished by activating each probe with a different phase, as a result of delaying the excitation time of each probe, the beam is pointed at an angle (figure 26). These new scanning principles have led to a variety of imaging/scan methodologies, their differences and explanations are listed next.

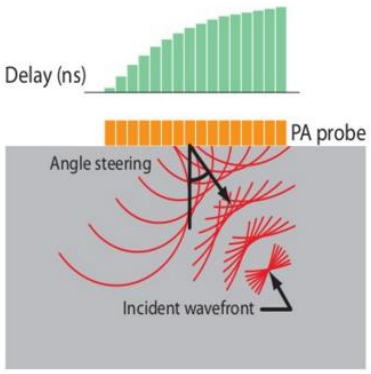

Figure 26: Phased array beam steering

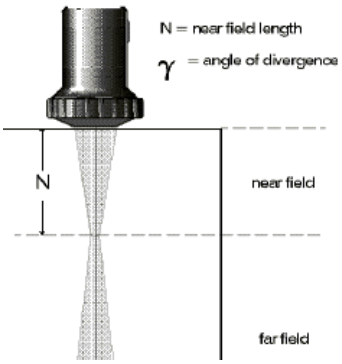

Figure 27: Focus depth

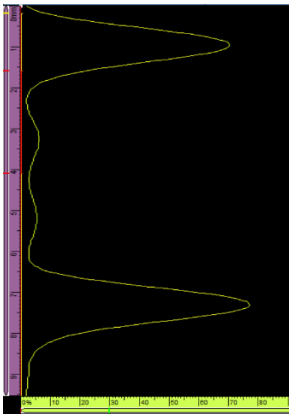

Figure 28: A-scan

A-scan: The A-scan is made by a single probe head, it presents the signal amplitude against the depth (Figure 28). In this example two reflections have returned to the probe, based on the reflection amplitude it can be estimated what causes the reflection. Note that by entering the specimen and hitting the backwall of the specimen a reflections will show up. As for this example, one peak is caused by the wave entering the material (front wall echo) and the wave reflecting at the back wall (back wall echo).

B-scan: The B-scan is made by a phased array probe. The B-scan measures the time of flight of each sound wave reflection and the amplitude. The combination of the depth and amplitude reflection results in a 2D representation of the vertical cross section (Figure 29). This scan is useful for finding the depth and thickness of a defect.

C-scan: The C-scan is a 2D representation over the surface of the specimen, the amplitude of the first reflections at each location is indicated in the surface map. The amplitude of the reflection needs to be above a certain threshold to be recognized as a reflection (defect). The colour map indicates the strength of the amplitude. A C-scan is effective way of visualizing the size and location of a defect. Note that the reflections caused by the wave entering the material is not taken into account.

D-scan: In principle, the D-scan is similar to the C-scan although now the depth of reflection is indicated instead of the amplitude. The depth is determined by converting the time of flight of the wave with the wave velocity, a colour map indicates the depth in the image.

S-scan: The S-scan or sectorial scan is made with a phased array probe when the beam is steered at a certain angle. This type of scan is particularly used for geometrical non-linear structures. The imaging principle is similar to the B-scan, the intensity of the wave reflection is indicated by a colour map

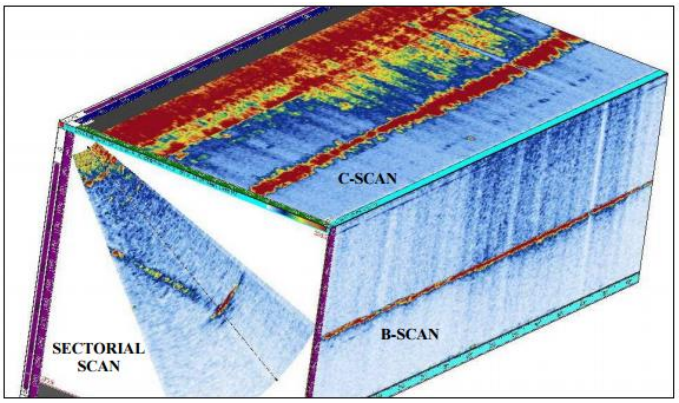

Figure 29: Ultrasound scanning methods [13]

High quality imaging with ultrasound scanning is dependent on a lot of parameter settings. Besides the settings, the image quality is influenced by the coupling between the probe and the material surface. The reliability and quality of the scan is dependent on these properties.

Two sets of settings can be distinguished for obtaining the right information when using an ultrasound scanner, the sound wave settings and imagining settings. The sound wave signal is mainly set by the focus depth, aperture, frequency, pulse width and energy. The aperture is the number of active probes per sound wave and this is only adjustable in case of phased array. The pulse width is length of wave in time.

The focus depth of the beam is limited by the near field (Figure 27). Each aperture, number of active probes per signal, has a unique near field range. This range can be calculated with the near field formula below, f is the frequency, C_l is the velocity of the longitudinal waves and D is the aperture of the probe (pitch x aperture). To improve the quality of the ultrasound analyses for thin panels, a wedge is used between the probe and the specimen to increase the time of flight. The formula [14] is already adjusted for the use of a wedge, $N_{CFRP\ contact}$ is the near field without using a wedge.

$$N_{CFRP} = N_{CFRP_{contact}} - L_{wedge}\frac{C_w}{C_L} \qquad N_{CFRP_{contact}} = \frac{D^2 f}{4C_l}$$

A beam with an aperture of 4 will always be unfocussed and an aperture of 8 for example has a maximum N_{CFRP} of $3.17\ \mathrm{mm}$. Higher apertures allow focussing up to 59.2 mm with use of a wedge. Cartier [15] stated that focussing at the exact depth of the defect can result in a more accurate scan, however the disadvantage of focussing is the loss of accuracy behind the focus point.

The main settings related to the image are the gain, time corrected gain (TCG) and the images type. These settings are less relevant when scanning thin panels, but they will be discussed later as well.

Methodology

The device used for the ultrasound scan of the aircraft panel is the Olympus OmniScan MX2 created by Olympus. As mentioned before, a probe wedge (Figure 30) is used to increase the time of flight of the wave. This increases the accuracy of the scan. The device specifications, probe type and wedge are listed below.

Device: Olympus OmniScan phased array (64 probe; 3.5L64-NW1)
Frequency: 3.5 MHz
Wedge: SNW1-0L-IHC-C Rev-C wedge (20 mm)

In order to acquire knowledge about the system and to gain experience, first the manual created by Cartier [15] is used. This manual includes two test specimen, one calibration panel and one with artificial defects. The artificial defects are made by integrated layers of backing film in between the composite layers. The user manual is useful for a first experience with the ultrasound scanner. This manual shows how to setup a first test and which settings are influencing the quality of the image. The effect of most settings are already discussed by Cartier. However, most settings are mainly focussed on scanning of thick panels. Secondly, the correctness of these settings is judged on the defect depth error and the defect size error for a thick specimen. The echo intensity and noise are not taken into account. Therefor the settings are evaluated and optimized for the functionality of scanning the aircraft panel. In appendix a: olympus omniscan settings, all settings are briefly discussed and optimized. Since there was no encoder present, the C-scanning is done manually as shown in figure 31. More details about manual scanning can also be found in the appendix.

Figure 30: Probe & Wegde

Figure 31: Manual C-scanning

Final settings

The optimized settings are applied and the scan image of the 2.35 mm section is shown in figure 32, this is the section of the aircraft where the damages are located. In the figure two echo's are visible, the first echo is caused by transition from the back wall of the wedge into the front wall of the panel. The second echo refers to the back wall of the panel. Note that the interval between the two echo's is narrow, this can conceal potential damages near the panel surface. The beam is focussed at the back wall of the panel, at 2.35 mm, with an energy of 40V, a 30 ns pulse width and an aperture of 8. In this particular image the coupling between the back wall of the wedge and the panel surface is good, since the first echo is weak. The gab in the back well op the panel refers to a different damage on the aircraft panel, more details about this gab are discussed in the appendix.

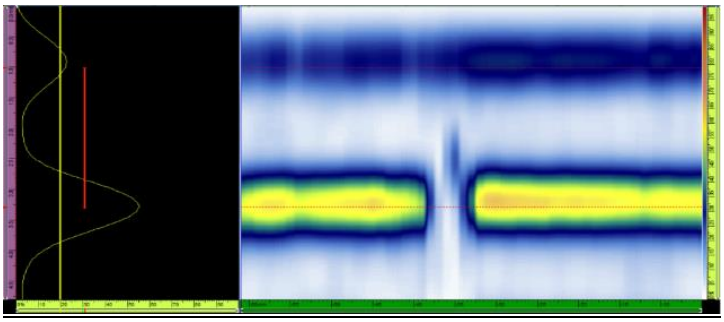

Figure 32: 2.35 mm DLR, PW 30 ns

Deformations air craft panel

The aircraft panel, created by DLR, is investigated. Two impact damages have been applied to the aircraft panel, both located at the thinnest section of the panel on top of the stringers (Figure 33, indicated in red). A spherical punch head is used to apply the impact, one damage is formed by a 10 mm punch head and the second one respectively 20mm. The applied impacts resulted in a local dent. A thin water film is used to improve the coupling between the probe and the specimen, however, these dents get stuffed with water. The signal propagation is distorted at these impact locations, causing a low energy reflection or even signal lost.

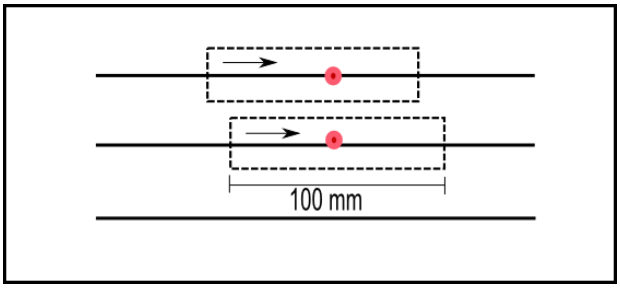

Figure 33:Scanning tracks

In the first scans there was no clear delamination visible around the middle of the cross section. Hence, a potential delamination should be located right underneath the bottom or top skin. The panel side with the stringers is taken as the bottom side. The top layer also did not show any signs of delamination, these results are added to the appendix. The bottom layers results are discussed in the next section in more detail.

A different C-scan imaging method is chosen as used in the appendix, because potential skin delamination may be concealed in the echo returning from the back wall of the panel. Therefor the amplitude of the echo is more useful as the depth. The amplitude is an indication for the fraction of energy that is returned. If a high fraction of the energy is returned by the echo, it could indicate a skin delamination. Note that this echo is also strongly influenced by the quality of the coupling.

Due to the production process of the panel, the plate is not entirely flat. The filler material used for connection the stringer to the plate cause scanning difficulties as well, a highly scaled picture of the deformation effect on the scanning accuracy is shown in figure 35. Scanning along the stringer results in figure 34, it shows that the areas with bad surface contact have a higher amplitude (yellow/orange areas) of the wedge back wall, because of bad coupling contact between the wedge and the panel surface. This figure clearly shows how the deformations affect the image and the reliability of the results.

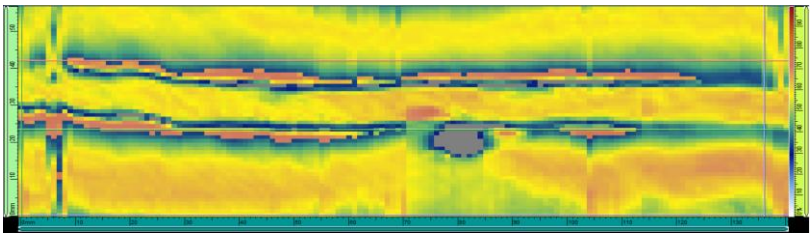

Figure 34: C-scan along stringer

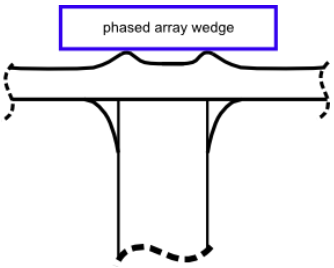

Figure 35: Stringer scan effect

Final scanning track

Potential stress concentration are expected to be located around geometry changes, hence the connection between the plate and stringer is more sensitive to delamination. The focus is now put on the second reflection peak (panel back wall), to scan for delamination's in this zone. The second reflection amplitude is represented in the C-scans next. As discussed, the panel is not entirely flat, therefor the scanning path is taken parallel to the stringers. This paths follows a constant line of deformation and thus experiences minimal changing coupling quality, in figure 33 the scanned area is indicated by the dashed box. To require a more constant wedge surface contact, a water film is created on the surface.

Figure 36 and figure 37 shows the images of the 4 scanning paths, the dents are indicated by a red circle and the piezo elements by black squares. The blue lines parallel to the stringer represent the edge of the filler material, other bleu/grey spots can be any kind of imperfection in the material structure. The yellow indicates a high amplitude of the panel back wall reflection

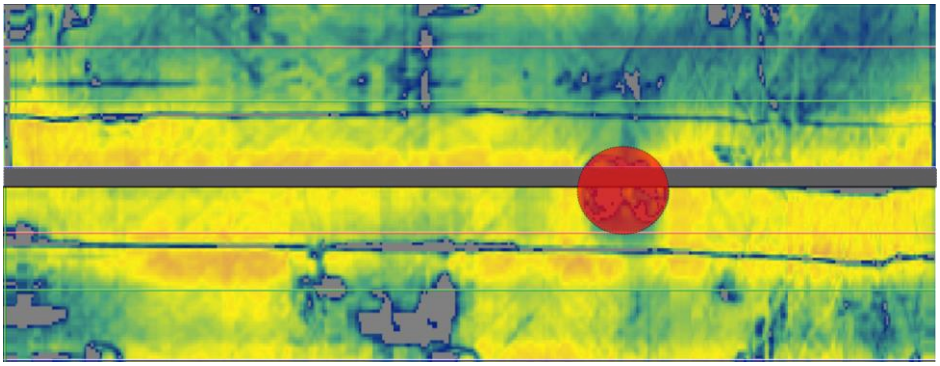

Figure 36: Scan Damage 20 mm

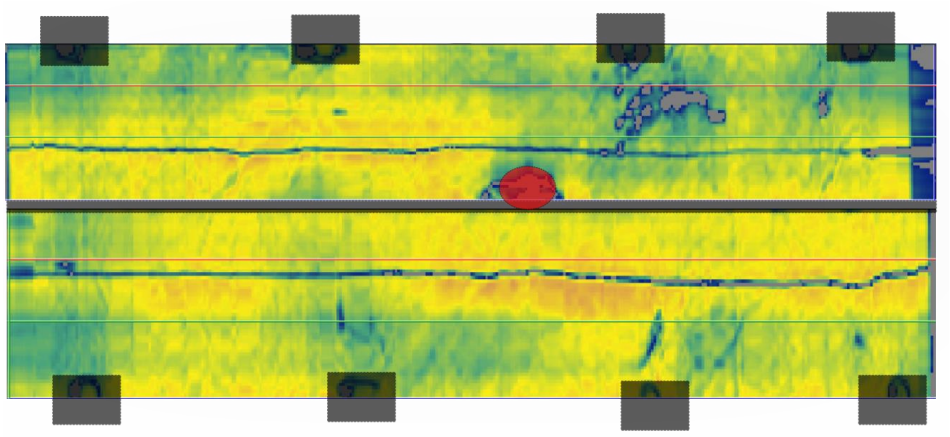

Figure 37: Scan Damage 10 mm

Some areas surrounding the 10mm damage show an increase in amplitude, however there is no significant prove that this is caused by delamination. The contact quality is still affecting the image too much, hence forming any conclusion based on these images is unreliable. Only some local material impurities or defects can be recognized by the grey spots. Also the results from A-scans or tapping with a coin did not show any signs of possible delamination. Considering there is no delamination hidden in the aircraft panel, the impact energy is possibly dissipated locally at the hitting point of the impact. Therefor the damage zone is scanned more locally.

Local impact area

S-scans make clear how the material structure locally is, figure 38 and figure 40 show the contours of the dents and are conform the findings by the human eye. Based on these images it can be stated that the material structure mainly contains local defects as a result of the impact application. However, this does not preclude the possibility of a delamination since the C-scans discussed earlier lack on reliability and visibility. In the event that the defects are just locally, the impact energy was possibly too high, causing all the impact energy to dissipate into the material destruction. In figure 39 the effect of different impact energy levels on the material structure are pointed out. Ideally, a medium impact energy results in delamination surrounding the impact point. For higher impact energy levels, more energy dissipates in the penetration of the material instead of delaminating.

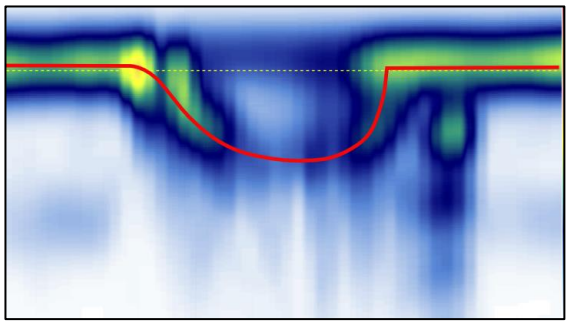

Figure 38: S-scan 10 mm dent

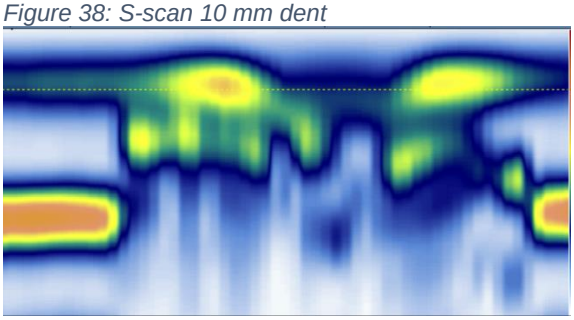

Figure 40: S-scan 20 mm dent

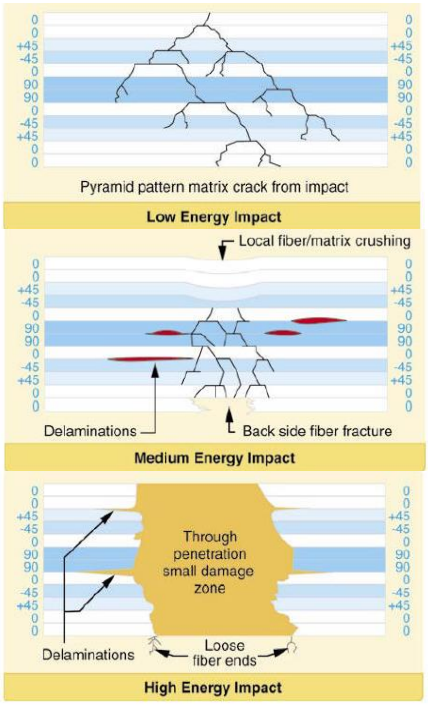

Figure 39: Impact energy levels [16]

Presence of voids and other damages

Although there are no clear delamination's detected surrounding the dent, the plate contains lots of imperfections or defects. These defects will as well influence the signal propagation of the guided Lamb waves. Imperfections are clearly visible in the C-scans shown before, the S-scan of one of the defects is taken as an example and presented figure 41. This could be a small air trap or wrinkle in the bottom surface of the plate.

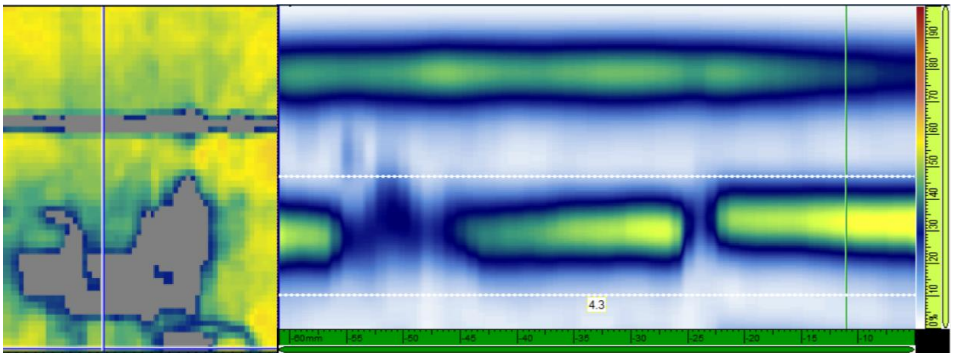

Figure 41: Defects in DLR panel

7. Conclusion & Outlook

Several aspects of the structural health monitoring method utilizing Lamb waves have been addressed in this research. Topics related to the method itself or to support research dedicated to this method. First of all the activation of Lamb waves using PWAS elements on a non-linear structure and a sandwich panel. Secondly the condition monitoring of the PWAS elements by measuring the susceptance. Lastly, ultrasound scanning is used for the damage identification of the defects on the aircraft panel.

The results related to the usage of different materials and geometries are mainly superficial and do not go into much detail. Nevertheless, non-linear geometries tend to have a negative influence on the propagation of Lamb waves, in the experiment the amplitude of the wave dropped significantly while passing the corner section. Besides non-linear geometries, limits of this method were found in the usage of different material structures. The sandwich structure, composed out of two glass fibre skins and a foam core showed interesting behaviour, a strong S-mode in combination with a disappearing A-mode. Regarding to this research, since only a small set of specimens with a few PWAS elements were tested, these results are not convincing. Further research has to point out whether these results are right and restrict the applicability of this method for sandwich structures with a foam core or non-linear geometries. Especially the applicability for non-linear structures is a critical aspect. To provide a proper SHM method for industry purposes all these difficulties have to be overcome.

Monitoring the state and condition of the PWAS elements based on susceptance is proven to be a simple and reliable method with much potential. This method indicated the debonding or lack of adhesive layer at PWAS 2 & 9, which could have affected the results found in the external research done by Loendersloot. The effect of debonding on the wave generation and sensibility is not investigated. One disadvantage of monitoring the susceptance is the need for an external electrical circuit, since it would be ideal to ultimately integrate the PWAS elements into the structure. The next step is to test this method on a larger scale, involving much more elements and in changing environmental conditions.

Ultrasound scanning was used to identify and characterize the damage caused by the applied impact series on the aircraft panel. The images following from the omniscanner did not meet the expectation of having delamination surrounding the panel – stringer connection. However, the S-scans made clear a significant defect directly underneath the impact hitting location. The material seems more or less penetrated at this point. Also other imperfections showed up in the scanner, these were not identified in more detail. To form reliable conclusions, different methods should be tested or the specimen has to be destructed.

References

[1] Z. Su, L. Ye, and Y. Lu, “Guided Lamb waves for identification of damage in composite structures: A review,” *J. Sound Vib.*, vol. 295, no. 3–5, pp. 753–780, 2006.

[2] K. Worden, “Rayleigh and Lamb Waves - Basic Principles,” *Strain*, vol. 37, no. 4, pp. 167–172, 2001.

[3] C. H. Zhong, A. J. Croxford, and P. D. Wilcox, “Remote inspection system for impact damage in large composite structure,” *Proc. R. Soc. A Math. Phys. Eng. Sci.*, vol. 471, no. 2175, pp. 20140631–20140631, 2014.

[4] R. a Badcock and E. a Birt, “The use of 0-3 piezocomposite embedded Lamb wave sensors for detection of damage in advanced fibre composites,” *Smart Mater. Struct.*, vol. 9, pp. 291–297, 2000.

[5] M. J. S. Lowe, “Matrix Techniques for Modeling Ultrasonic-Waves in Multilayered Media,” *Ieee Trans. Ultrason. Ferroelectr. Freq. Control*, vol. 42, no. 4, pp. 525–542, 1995.

[6] S. Kim and U. Lee, “Effects of Delamination on Guided Waves in a Symmetric Laminated Composite Beam,” vol. 2014, 2014.

[7] TiePie engineering, “Handyscope HS4 key specifications.” [Online]. Available: http://www.tiepie.com/en/products/Oscilloscopes/Handyscope_HS4/Key_specifications.

[8] T. Saar, “Robust piezo impedance magnitude measurement method,” *Elektron. ir Elektrotechnika*, vol. 7, no. 7, pp. 107–110, 2011.

[9] J. K. J. Kim, B. L. Grisso, J. K. Kim, D. S. H. D. S. Ha, and D. J. Inman, “Electrical modeling of Piezoelectric ceramics for analysis and evaluation of sensory systems,” *2008 IEEE Sensors Appl. Symp.*, pp. 122–127, 2008.

[10] S. Bhalla and C. K. Soh, “Electromechanical Impedance Modeling for Adhesively Bonded Piezo-transducers,” *J. Intell. Mater. Syst. Struct.*, vol. 15, no. 12, pp. 955–972, 2004.

[11] I. Buethe, M. Moix-bonet, P. Wierach, C. Fritzen, and Paul-bonatz-strasse, “Check of Piezoelectric Transducers Using the Electro-Mechanical Impedance,” *EWSHM - 7th Eur. Work. Struct. Heal. Monit.*, pp. 748–755, 2014.

[12] NDT Resource Centre, “Reflection and Transmission.” [Online]. Available: https://www.nde-ed.org/EducationResources/CommunityCollege/Ultrasonics/Physics/reflectiontransmission.htm .

[13] C. Chartier, “Phased Array Ultrasonic Detection & Sizing of In-Service Cracks in Heavy Walled Reactor Nozzles - Part 1,” *NDT.net*, pp. 1–9, 2009.

[14] D. Terminal, “N° 4 •,” no. January, pp. 0–7, 2001.

[15] B. Cartier, “Phased array ultrasonic inspection of advanced composite laminates,” University of Auckland.

[16] “Types of Aircraft Construction.” [Online]. Available: http://www.waybuilder.net/free-ed/Resources/15-Transportation/Aviation/AircraftStructure.asp?iNum=3.

Appendix A: Olympus Omniscan settings

The aircraft panel already has some damages from previous use, on the topside there are small gutters over the whole length of the panel. The C-scan made by DLR (figure 42) before the impact load gives a good representation of the gutters, these are the white line perpendicular to the stringers. The damage is also clearly visible by the human eye, hence it is not classified as a barely visible damage. Despite the fact that the damage is classified different, it is helpful for tuning the right settings for this panel. The panel can be divided in three different thickness sections. On the lefts side, the dark blue section is 6.2 mm thick, the middle section is 2.35mm and the right side is 4.2 mm.

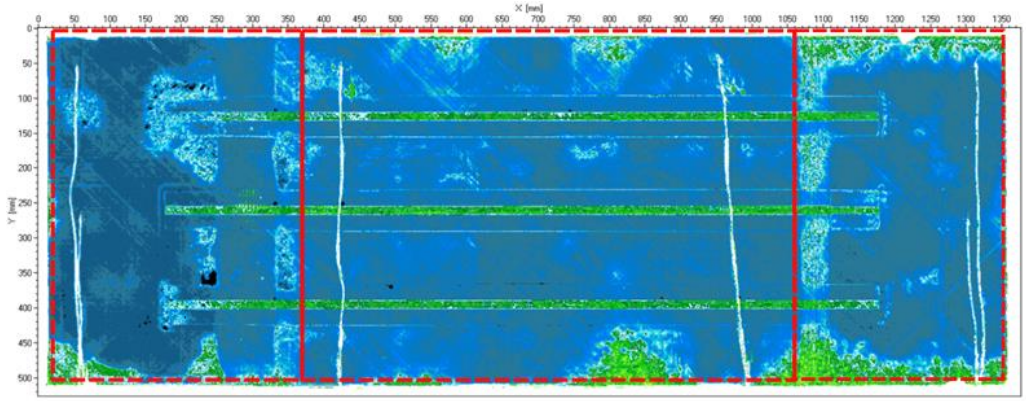

Figure 42: C-scan aircraft panel by DLR

First the 6.5, 4.2 and 2.35 mm thick sections are analysed for a quick quality indication (figure 43, figure 44, figure 45). On the left side of the images the A-scan is shown, the first echo refers to the back wall of the wedge, the second echo refers to the back wall of the specimen. Initially an unfocussed beam with an aperture of 4 is used. Remark, in the scan image there is a gab in the back wall reflection, this gab represents the damage (gutter) on the panel. When the beam is focussed at this gutter, the beam gets reflected all directions, no proper signal is returned to the probe.

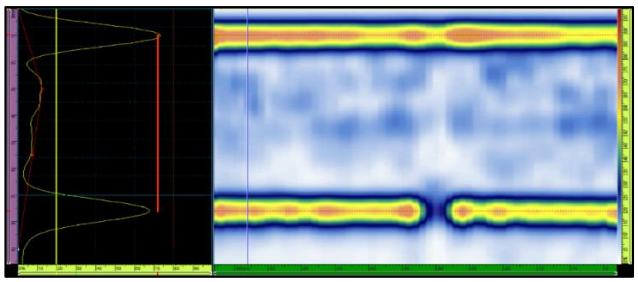

Figure 43: 6,5 mm section DLR panel, Aperture 4

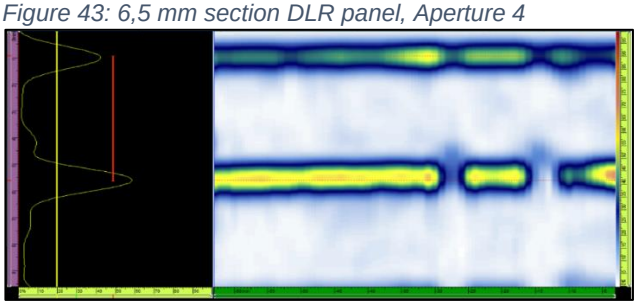

Figure 44: 4.2 mm Section DLR panel, Aperture 4

The scans of the thinnest plate section (2.35 mm) show a small interval between the two reflections. The reflection peaks cover a large part of the image in the A and S-scan. It means that the sound wave length is large compared to the time of flight. Due to this small time interval it is hard to detect defects over the thickness, since flaws usually reflect only a small part of the energy. In that case, defects can be concealed in one of the reflections. In all the S-scan, there is also a variation in the amplitude of the reflection noticeable, this is caused by the coupling quality of the water between the wedge and the specimen. Good coupling decreases the peak amplitude.

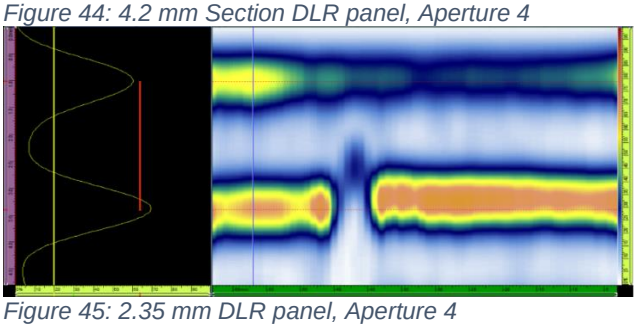

Figure 45: 2.35 mm DLR panel, Aperture 4

Wave velocity

The wave velocity is used to convert the time of flight of echo into distances. By measuring the distance between the first and second peak in the A-scan, the thickness of the specimen is estimated at 6.6 mm. The error between the thickness measured by the scanner and the real thickness is mainly caused by the estimated wave velocity in the material, the standard wave velocity setting for composites is 3000 m/s. This can vary a bit with the layup structure, resin/fibre fraction etc. The calibration of the right velocity is done on different thicknesses, for the air craft panel, the 4,2 and 6,35 mm thick sections are used, resulting in a wave velocity of 2981 m/s.

Pulse width

The pulse width is length of the sound wave signal, in the standard settings the pulser time is 142 ns. Since this test specimen is relatively thin and hence the time of flight is short, it is beneficial to decrease the pulser width. The pulse width is also related to the width of the reflection peak. A shorter pulse width results in a reduction in peak width, however dispersion always causes the width to increase. Dispersion is the effect of separation of high and low frequency waves when propagating through a material, directly increasing the peak width. In the A-scan the back wall reflection peak width is estimated at 1.38 mm. A reduction of the pulse width to 30 ns should lead to a decrease in peak with, which is beneficial for the detection of defects. In practise, the peak did not change much in size, however, it increased in accuracy. The C and A-scan are shown in figure 46, the gab is bigger and clearer in this image compared to figure 43. The width of peak in the S-scan was estimated at 0.84 mm.

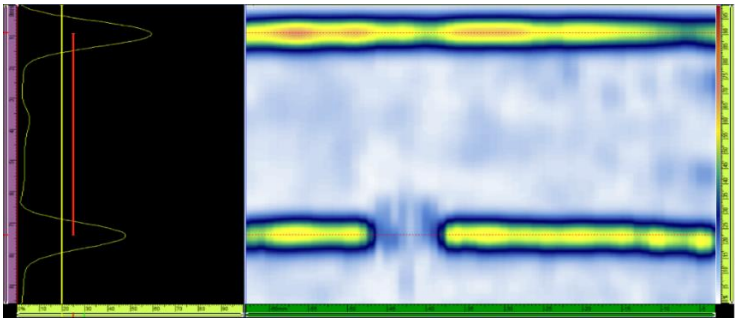

Figure 46: 6.23 mm, PulseWidth 30 ns

Signal energy

The energy of the signal parameter can be set to 40, 80 or 115 Volts. Increasing the energy results in a higher energy reflection at a defect, which leads to a stronger echo. This parameter has however not much influence, since the strength of the echo is also adjusted by the gain. If the energy is set low, the gain is set higher to get a clear image and the other way around. Changing the energy of the pulse has almost no effect on the scan. Materials with high attenuation ratios or thickness could possibly benefit from increasing the energy, since echoes cover larger distances and are automatically more attenuated. More important in this test, is the coupling between the wedge and the surface. If the coupling is good, the back wall echo of the wedge decreases, while the back wall echo of the plate increases.

Focal law

Finally the focal law parameters have to be tuned, the previous scans are done with an aperture of 4 and this always results in an unfocussed beam. Focussing the beam at specific depths can highlight local defects or imperfection. A trial shows the effect of different focus depths, the aperture is 16 and the specimen thickness is 6.35 mm, resulting in figure 47 and figure 48. Focussing on a specific depth, increases the accuracy of the reflections in that area. However, the echoes behind the focussing depth will get unclear due to the pressure decay outside of the unfocussed region. In the figure below, two different focus depths are tested, one focussing at the back wall and the second one focussed at a depth of 11mm. For thin panels it is beneficial to focus on the back wall, it has a positive effect on the back wall visualization without losing accuracy in the beginning.

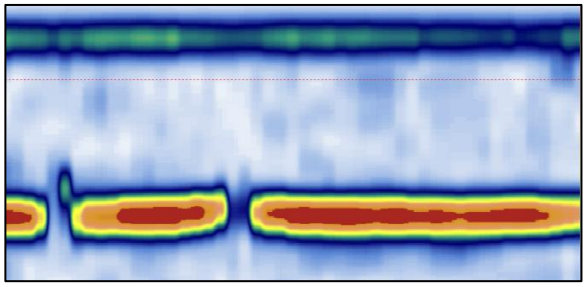

Figure 47: Focal law, Aperture 16, 6 mm focus

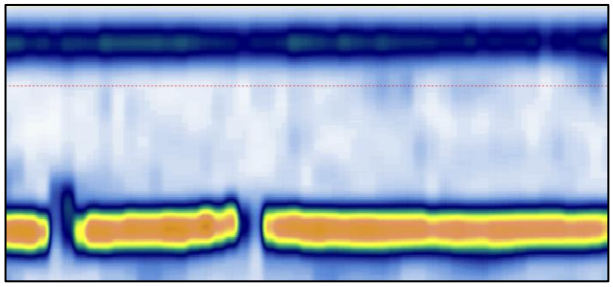

Figure 48: Focal law, Aperture 16, 11 mm focus

Frequency

The frequency of the pulse is not a variable parameter, although this would benefit for small thicknesses. Lower frequencies have a higher penetration depth as higher frequencies. Higher frequencies do have a better resolution and focal sharpness[12]. A further increase in frequency (Olympus: 3.5MHz) should probably be beneficial.

Gain and TCG

The gain is set to 2, sound waves in thin specimens have a short time of flight, hence the signal is not much attenuated and the amplitude is high. A time corrected gain (TCG) is only beneficial for thick specimens, this feature increases the gain for reflections returning from deeper in the material. These deeper echoes have a higher attenuation ratio, because their path is longer.

C-scan

The C-scan shows a map consisting of the first echo's amplitude at each location. To conduct a C-scan over a large area, the reflection data and location is linked to make a surface map. Location control is done by an encoder, although the encoder is not available for this research. Nevertheless, it is possible to set up a small area C-scans with the omniscanner in combination with the phased array probe. However, in this case the C-scan requires a constant motion velocity in linear direction since the location cannot be recorded. Manually controlling the movement speed of the probe has the consequence that the final image may be different as in reality.

In the Omniscan, Gate A, under Gates/Alarms sets the sensitivity for flaw detection in the C-scan. By increasing the threshold, ignores the reflection peaks below that threshold. Balancing this parameter is important, it determines what size/type of defects shows up in the image. The threshold is set to a certain percentage of the backwall reflection. In figure 49 the threshold is set at 28%. If a peak exceeds the threshold line, it is considered as a defect or imperfection. The time of flight is used to determine defect depth, the depth is indicated with a colour palette. The colour palette can be changed under 'Display', 'properties'.

The C-scan shown at the bottom of the figure is made by hand. In the 'Scan' menu, under 'Inspection', the type is set to 'One-line scan' and the scan mode is set to 'Time'. This is the only option for scanning manually. The last setting is adjusting the scanning speed, scanning manually can be done properly at a speed of 1 to 3 mm/s. Using a scale alongside the track and manually counting gives the most accurate result. For the figures a path length of 100 mm chosen.

The thicker plate section (6.3 mm) are used again in attempt to fine tune the settings of the omniscan. Once again the gutters show up clearly in the image (figure 49) as white lines. The white colour represents no thickness or loss of signal, resulting from the fact that the signal is scattered. The green area represents a delamination or imperfections at a depth of 3mm. These images show that the specimen already contains quite a lot of damages.

In figure 50, a C-scan is made of the 4.3 mm section. This panel side has a similar damage, the gutter can be seen in the lower section of the figure. Halfway the C-scan the colour changes due to the thickness change. The thickness within each section is also not entirely constant.

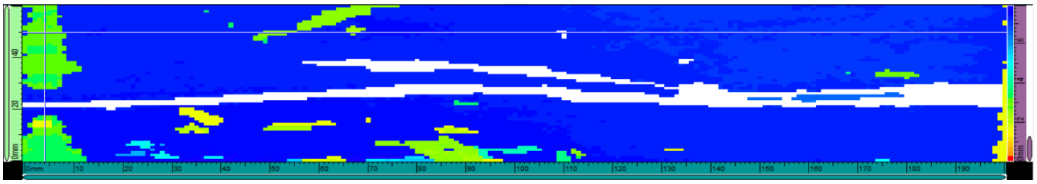

Figure 49: C-scan 6.35 mm section

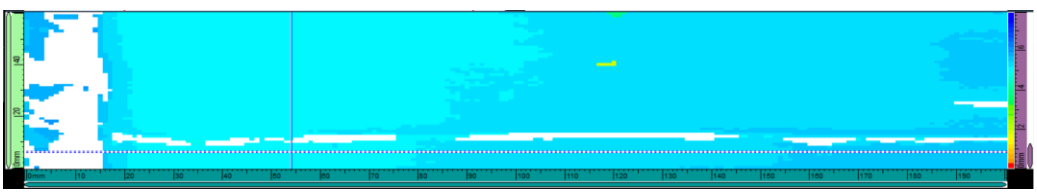

Figure 50: C-scan, 4.3 mm section

Top skin C-scan

In figure 51, the first echo amplitude is plotted. The blue colour indicates that most of the energy is returned by the back wall of the panel. The grey area indicates signal lost, no proper signal is returned to the probe. The yellow/orange areas can be an indication of skin delamination or bad coupling. Since the plate top surface lost its flatness by the applied impacts, it is hard to form any conclusions based on this image. Possibly also the area surrounding the dent is plastically deformed. The image is also influenced by the manual scanning technique, the scanning velocity is not constant over the track, as a result the dimensions in the scan are not exact and the impact location is not a perfect circle.

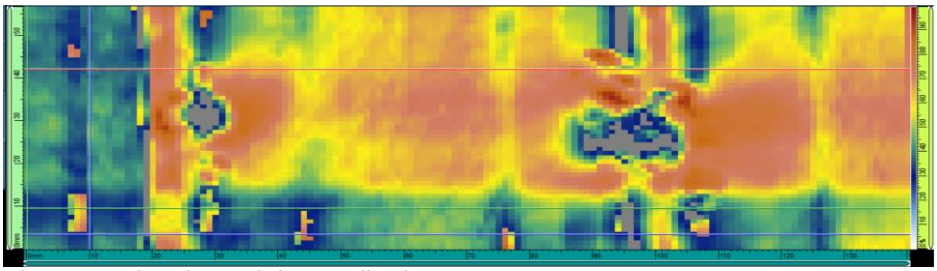

Figure 51: Aircraft panel, front wall echo, C-scan